American Journal of Emergency Medicine 35 (2017) 1082–1089

Contents lists available at ScienceDirect

American Journal of Emergency Medicine

journal homepage: www.elsevier.com/locate/ajem

Original Contribution

Cardioprotective effect of nicorandil against myocardial injury following cardiac arrest in swine

Li-Ning Liang, Xia Zhong, Yi Zhou, Zhi-Qiang Hou, Hao-Ran Hu, Fang-Fang Zhu, Ji-Bin Chen, Xian-Fei Ji *, De-Ya Shang *

Department of Emergency, Shandong Provincial Hospital affiliated to Shandong University, No. 324, Jingwu Road, Jinan 250021, Shandong, China

ARTICLE INFO

Article history:
Received 13 November 2016
Received in revised form 27 February 2017
Accepted 28 February 2017

Keywords:
Cardiac arrest
Myocardial injury
Nicorandil
Swine

ABSTRACT

Introduction: Nicorandil, a vasodilatory drug used to treat angina, was reported to protect against myocardial ischemia-reperfusion injury in various animal models. However, its cardioprotective action following cardiac arrest is unknown. We examined the cardioprotective effects of nicorandil in a porcine model of cardiac arrest and resuscitation.

Methods: Ventricular fibrillation was induced electrically for 4 min in anesthetized domestic swine, followed by cardiopulmonary resuscitation. Sixteen successfully resuscitated animals were randomized to saline control (n = 8) or nicorandil (n = 8) groups. Nicorandil (150 μg/kg) was administered by central intravenous injection at onset of restoration of spontaneous circulation (ROSC), followed by 3 μg/kg/min infusion until reperfusion end. Sham-operated animals received surgery only (n = 4). Hemodynamic parameters were monitored continuously. Blood samples were taken at baseline, 5, 30, 180, and 360 min after ROSC. Left ventricular ejection fraction was assessed by echocardiography at baseline and 6 h after ROSC. The animals were euthanized 6 h after ROSC, and the cardiac tissue was removed for analysis.

Results: 6 h after ROSC, nicorandil had significantly improved all hemodynamic variables (all $P < 0.05$) except the maximum rate of left ventricular pressure decline and heart rate ($P > 0.05$) compared with the control group. Control animals showed elevated cardiac troponin I and lactate levels compared with sham animals, which were significantly decreased following nicorandil treatment ($P < 0.05$). In the saline control group, the adenosine triphosphate (ATP) content was largely reduced but subsequently rescued by nicorandil ($P < 0.05$). Histopathologic injury was reduced with nicorandil treatment. Nicorandil reduced cardiomyocyte apoptosis as evidenced by reduced terminal deoxynucleotidyl transferase dUTP nick-end labeling (TUNEL)-positive cells, decreased Bax and caspase-3 expression, and increased Bcl-2 expression in the myocardium (all $P < 0.05$).

Conclusion: Nicorandil exhibited cardioprotective effects on myocardial injury following cardiac arrest *via* improvement in post-resuscitation myocardial dysfunction and energy metabolism, reduction in myocardial histopathologic injury, and antiapoptotic effects.

1. Introduction

Ventricular fibrillation (VF) is the primary cause of sudden cardiac events [1,2]. Despite significant progress in resuscitation and improved restoration of spontaneous circulation (ROSC), the morbidity and mortality from cardiac arrest (CA) remains high [3]. Indeed, the overall survival to discharge remains at 9.6–17% for out-of-hospital cardiac arrest and in-hospital cardiac arrest [4,5]. Post-ischemic myocardial dysfunction is the leading cause of the high mortality observed during the 72 h after resuscitation from cardiac arrest [6]. Although this cardiovascular dysfunction is considered transient [7,8], there is an association of arterial hypotension and low cardiac output (CO) with poor outcome in post-cardiac arrest patients [7,9,10]. Interventions targeting the improvement of postarrest myocardial dysfunction may produce clinical benefits.

Nicorandil, an ATP-sensitive potassium (KATP) channel opener and nitric oxide donor, is currently used as a standard drug for the treatment of coronary artery disease in the clinical setting. Evidence has demonstrated that it improves the recovery of the post-ischemic contractile dysfunction of the heart and reduces the infarct size after coronary artery occlusion and reperfusion in basic and clinical studies [11]. Unlike focal myocardial ischemia as a result of coronary artery occlusion, the entire myocardium is affected in cardiac arrest, leading to transient but global changes in cardiac systolic and diastolic function. Takarabe et al. [12] revealed that nicorandil attenuated myocardial reperfusion

* Corresponding authors at: Department of Emergency, Shandong Provincial Hospital affiliated to Shandong University, 324 Jingwu Road, Jinan, Shandong, 250021, China.
E-mail addresses: Sdslyyjxf123@163.com (X.-F. Ji), Sdslyysdy123@163.com (D.-Y. Shang).

http://dx.doi.org/10.1016/j.ajem.2017.02.051
0735-6757/

Table 1
Resuscitation outcomes.

Outcomes	Saline (n = 8)	Sham (n = 4)	Nicorandil (n = 8)
Number of shocks	1.25 ± 0.46*	0	1.13 ± 0.35#
Total adrenaline dose (mg)	0.12 ± 0.022	0	0.06 ± 0.017
Time to ROSC (min)	2.50 ± 0.93*	0	2.25 ± 0.71#
Energy of shock (J)	200 ± 92.58*	0	175 ± 70.71#

* $P < 0.05$ *vs.* saline group.
\# $P < 0.05$ *vs.* sham group.

injury following prolonged cardioplegic arrest in an isolated rabbit heart model. However, there is limited data regarding the application of nicorandil in models of cardiac arrest and resuscitation, which is characterized by complex pathophysiological changes. In the present study, we investigated the protective effects of nicorandil on myocardial injury in a swine model of cardiac arrest and resuscitation induced by 4-min untreated VF.

2. Materials and methods

2.1. Animals

The animal experimental protocol was approved by the Animal care and use Committee of Shandong Provincial Hospital. All animals received humane care in compliance with the Guide for the Care and Use of Laboratory Animals published by the National Institutes of Health. In this study, twenty male Landrace domestic pigs (25 ± 2 kg) were used and randomized into three groups: sham operation group (sham group, n = 4), saline control group (saline group, n = 8) and nicorandil group (nicorandil group, n = 8). All animals were maintained in a specific pathogen-free environment in our facility, and were fed with standard chow and had free access to water. Room temperature was adjusted to 26 °C. All efforts were made to minimize the animals' suffering.

2.2. Animal preparation

All pigs were fasted overnight with free access to water. After premedication midazolam (0.5 mg/kg i.m.), anesthesia was induced by ear vein injection of propofol (1.0 mg/kg) and maintained with sodium pentobarbital (8 mg/kg i.v.) at hourly intervals on a surgical plane of anesthesia. Additional doses of sodium pentobarbital (8 mg/kg) were administered when animals awakened or showed signs of restlessness. Anesthetic drugs were not administered for an interval of 30 min prior to experiments.

All animals were intubated with a 7.0-mm cuffed tracheal tube (Mallinckrodt Critical Care, Glens Falls, NY, USA). Animals were mechanically ventilated with a volume-controlled ventilator (8417801-22; Dräger Medical GmbH, Lübeck, Germany) with a tidal volume of 12 ml/kg and FiO_2 of 21%. End-tidal carbon dioxide ($ETCO_2$) was monitored with an infrared capnometer (Pulsion Medical Systems SE, Munich, Germany) connected to a Philips monitor (M8003A; Philips Medizin Systeme Boeblingen GmbH, Boeblingen, Germany). Respiratory frequency was adjusted to maintain $ETCO_2$ between 35 and 40 mm Hg before cardiac arrest and after resuscitation.

Fluid loss was replaced by infusing 30 ml/kg of acetated Ringer's solution during the first hour of preparation, followed by continuous infusion of 2.5% glucose electrolyte solution at 8 ml/kg/h and lactated Ringer's solution at 20 ml/kg/h. A conventional lead II electrocardiogram was continuously monitored during instrumentation and throughout the study protocol by applying five adhesive electrodes to the shaved skin of the proximal right and left, upper and lower limbs and the upper abdomen. A thermodilution catheter (4F; Pulsion Medical Systems SE) was inserted into the left external jugular vein to measure CO. The catheter allowed discontinuous measurement of CO by injecting 15 ml of ice-cold saline into the proximal port of the central venous catheter. The mean of three consecutive measurements was used for determination of CO. A saline-filled central venous catheter (6 Fr) was inserted in the right internal jugular vein for blood sampling.

To induce VF, a pacing catheter (5 Fr) was advanced from the right internal jugular vein into the right ventricle. Left ventricular function was measured using a fluid-filled polyurethane catheter (introduced from the right carotid artery to the left ventricle) to determining the maximum rate of left ventricular pressure increase (dp/dtmax) and the maximum rate of left ventricular pressure decline (−dp/dtmax) (BL-420F Data Acquisition & Analysis System; TME Technology Co., Ltd., Chengdu, China). A thermistor-tipped catheter (4F; Pulsion Medical Systems SE) was inserted into the right femoral artery for measurement of arterial pressure and core body temperature. The arterial catheter was connected the PiCCO system (PiCCO plus v.6.0 software; Pulsion Medical Systems SE), and signals were processed to determine mean arterial blood pressure (MAP) and blood temperature. Core body temperature was monitored continuously *via* the arterial catheter.

Normothermic body temperature was maintained at 37.5 ± 0.5 °C using a cooling/warming blanket (Model P&C-A; Hengbang Products, Beijing, China) throughout the entire experiment. All catheters were calibrated before application and their positions verified by presence of typical pressure waves. All catheters were flushed with isotonic saline containing 5 IU/ml heparin (3 ml/h) to prevent obstruction. All hemodynamic parameters were monitored using a Philips monitor.

2.3. Experimental protocol

After the operation, animals were equilibrated for 30 min to achieve a resting level, and baseline measurements and blood samples were then performed. Using a programmed electrical stimulation instrument (DF-5A; KaiFeng Henan Instrument Company, Kaifeng, Henan, China), VF was induced in 18 of 22 pigs using S1S2 mode (300/200 ms), 40 V, 8:1 proportion, and a 10-ms step length to provide a continuous electrical stimulus. VF was confirmed by presence of a characteristic electrocardiogram waveform and a rapid decline in mean aortic pressure toward zero [3]. Mechanical ventilation was stopped after successful induction of VF. After 4 min of untreated VF, cardiopulmonary resuscitation (CPR) was performed manually at 100–120 compressions/min with mechanical ventilation at an FiO_2 of 100%, minimizing interruptions in chest compressions, and ensuring chest compressions of adequate depth, in accordance with the 2015 American Heart Association Guidelines for Cardiopulmonary Resuscitation and Emergency Cardiovascular Care [13]. After 2 min of CPR, defibrillation (LIFEPAK20; Medtronic, Inc.) was first attempted using 150 J. If VF persisted, another 2-min CPR was resumed, followed by bolus epinephrine (0.02 mg/kg) and 200 J defibrillation for all subsequent attempts. If required, additional doses of epinephrine were administered every 3 min until ROSC was achieved.

ROSC was defined as maintenance of systolic blood pressure at 50 mm Hg for 10 min. If spontaneous circulation was not restored within 30 min, the animal was considered dead.The sixteen successfully

Table 2
Baseline characteristics.

Characteristic	Saline (n = 8)	Sham (n = 4)	Nicorandil (n = 8)	*P*-values
Weight (kg)	25.38 ± 1.41	24.25 ± 1.26	24.88 ± 1.38	0.419
HR (beats/s)	121.88 ± 5.17	125.50 ± 3.87	121.50 ± 4.44	0.361
$ETCO_2$ (mm Hg)	36.75 ± 1.67	37.25 ± 2.06	36.88 ± 1.55	0.890
PH value	7.42 ± 0.02	7.42 ± 0.03	7.42 ± 0.02	0.745
Temperature (°C)	37.51 ± 0.24	37.45 ± 0.21	37.49 ± 0.27	0.920
MAP (mm Hg)	115.38 ± 4.27	116.25 ± 4.03	116.75 ± 2.38	0.743
CO (l/min)	4.46 ± 0.19	4.52 ± 0.15	4.53 ± 0.16	0.737
dp/dtmax (mm Hg/s)	4628.75 ± 195.92	4562.50 ± 274.39	4615 ± 185.32	0.871
−dp/dtmax (mm Hg/s)	3938.75 ± 273.26	4067.50 ± 264.24	3932.50 ± 251.5	0.674

Table 3
Left ventricular ejection fraction.

Group	Baseline	ROSC 6 h
Sham	0.75 ± 0.008	0.74 ± 0.008
Saline	0.75 ± 0.006	0.56 ± 0.006*,#
Nicorandil	0.75 ± 0.007	0.63 ± 0.009*,#,▲

* $P < 0.05$ *vs.* baseline.
\# $P < 0.05$ *vs.* sham group.
▲ $P < 0.05$ *vs.* saline group.

resuscitated pigs were randomized (envelope method) to receive central venous injection of saline (saline control group, n = 8) or nicorandil (nicorandil group, n = 8) (Beijing SHKB Pharmaceutical Co., Ltd.) at ROSC onset. Four additional pigs used as sham controls were anesthetized and instrumented, but VF was not induced. Researchers were blinded to the drug treatments until data collection was complete.

After successful resuscitation, animals underwent intensive care for 6 h, and mechanical ventilation was resumed using pre-cardiac arrest settings, except that FiO_2 was reduced to 30 min after ROSC to avoid hyperoxia. Blood samples were collected at 5 min, 0.5, 3, and 6 h after ROSC, and hemodynamic data were collected hourly during the observation period. Echocardiographic data were collected before animals were euthanized (pentobarbital 150 mg/kg i.v.), and samples of the cardiac tissue were collected. Autopsy was routinely performed to document potential thoracic and abdominal cavity injury during CPR.

2.4. Hemodynamic measurements

Hemodynamic parameters, including heart rate (HR), MAP, CO, dp/dtmax, and −dp/dtmax, were continuously displayed and recorded with a biosignal acquisition system throughout the experiments. Left ventricular dp/dtmax was used to estimate isovolemic contractility. The −dp/dtmax was used to estimate of myocardial relaxation. CO was measured with the thermodilution technique. Data were recorded at baseline, 30 min, 1, 2, 3, 4, 5, and 6 h after ROSC.

2.5. Measurements of CO_2, pH, lactate, cTnI and ATP

One set of blood samples was processed immediately after collection for temperature-corrected measurement of oxygen, CO_2, pH, and lactate using an automatic blood gas analyzer (GEM 4000; Instrumentation Laboratory GmbH, Munich, Germany) at baseline, 5, 30, 180, and 360 min after ROSC. To evaluate myocardial injury, venous blood samples were collected and cardiac-specific troponin-I (cTnI) immediately assessed using an AQT90 FLEX immunoassay analyzer (Radiometer, Shanghai, China) at baseline, 5, 30, 180, and 360 min after ROSC. Adenosine triphosphate (ATP) was measured using a porcine adenosine triphosphate (ATP) ELISA kit from Wuhan ColorfulGene Biological Technology Co., LTD.

2.6. Cardiac function study by echocardiography

As a quantitative measure of myocardial contractile function, left ventricular ejection fraction (EF) was assessed using a 2.5-MHz transthoracic transducer with echocardiography (CLOVER; Wisonic, Shenzhen, China) at baseline and 360 min after ROSC. Data were reviewed and confirmed separately by two investigators. Images were obtained in long-axis parasternal views with two-dimensional and M-mode modalities. EF was obtained by the modified Simpson method at the level of the papillary muscles. Interpretation of echocardiograms was performed by investigators blinded to the groups.

2.7. Tissue morphology and ultrastructure

At the end of experiments, cardiac apex of left ventricle was collected and immediately fixed in 4% paraformaldehyde and glutaraldehyde solution at 4 °C. Sections were prepared following routine procedures. Myocardial tissue morphology was assessed by light microscopy (Olympus, Japan), and ultrastructure assessed by transmission electron microscopy (JEOL, Japan). Histological evaluation was performed by experienced pathologists blinded to the groups.

2.8. TUNEL assay

Apoptosis of cardiomyocytes was evaluated by terminal deoxynucleotidyl transferase-mediated dUTP nick end labeling (TUNEL) staining, which was carried out strictly according to the manufacturer's instructions (bioswamp). After deparaffinization and rehydration, the sections were treated with 10 mmol/l protease K for 15 min. The slides were immersed in a TUNEL reaction mixture for 60 min at 37 °C in a humidified atmosphere in the dark. Slides were then incubated with converter-POD for 30 min to stain nuclei, followed by analysis with microscopy. The TUNEL index (%), which was to evaluate the apoptosis index of the TUNEL-stained heart tissues, is the average ratio of the number of TUNEL-positive cells divided by the total number of cells. Eight randomly selected microscopic fields (400× magnification) of TUNEL-stained slices were counted for each sample, and the average value was calculated.

2.9. Western blot analysis

The expressions of caspase-3, Bax and Bcl-2 were detected using Western Blot. Myocardial tissues were homogenized in ice-cold RIPA buffer containing PMSF and the supernatant was harvested by centrifugation (4 °C, 12,000 r/min, 15 min). Tissue total protein concentrations were determined by a BCA protein assay kit (bioswamp). The protein lysates (10 μg) were loaded onto 12% sodium dodecyl sulfate poly acrylamide gel electrophoresis (SDS-PAGE), and electrotransferred to PVDF membranes, and blocked in 5% nonfat milk sealing fluid. Membranes were incubated overnight using primary antibodies (caspase-3 (abcam, no.ab4051) diluted to 1:500, Bcl-2 (abcam, no.ab32124) diluted to 1:1000, and Bax (abcam, no.ab32503) diluted to 1:5000) at 4 °C. After washing 3 times with PBST, the membrane was incubated to horseradish peroxidase-conjugated secondary antibodies (goat anti-rabbit) for 1 h. The protein band was visualized using an enhanced chemiluminescence (ECL) kit and the density of each band was quantified using a western blotting detection system (Tanon-5200; Tanon Science & Technology Co., Ltd., Shanghai, China). GAPDH protein served as an internal calibration.

Table 4
Serum cardiac-specific troponin-I concentrations (ng/ml).

Group	Baseline	ROSC 5 min	ROSC 30 min	ROSC 180 min	ROSC 360 min
Sham	0.042 ± 0.018	0.042 ± 0.012	0.041 ± 0.012	0.041 ± 0.012	0.041 ± 0.012
Saline	0.041 ± 0.013	0.279 ± 0.097*,#	0.421 ± 0.051*,#	2.638 ± 0.297*,#	2.275 ± 0.198*,#
Nicorandil	0.041 ± 0.013	0.244 ± 0.072*,#	0.365 ± 0.078*,#	1.255 ± 0.252*,#,▲	1.019 ± 0.236*,#,▲

Inspection level required corrected. $\alpha' = 0.05/10 = 0.005$.
* $P < 0.005$ *vs.* baseline. $\alpha'' = 0.05/3 = 0.017$.
\# $P < 0.017$ *vs.* sham group.
▲ $P < 0.017$ *vs.* saline group.

Table 5
Serum lactate concentration (mmol/l).

Group	Baseline	ROSC 5 min	ROSC 30 min	ROSC 180 min	ROSC 360 min
Shamm	1.18 ± 0.22	1.08 ± 0.19	1.08 ± 0.19	1.08 ± 0.19	1.08 ± 0.19
Saline	1.25 ± 0.20	7.85 ± 0.57*,#	5.63 ± 1.38*,#	1.73 ± 0.79	1.05 ± 0.30
Nicorandil	1.25 ± 0.18	5.90 ± 1.02*,#,▲	3.83 ± 0.88*,#,▲	1.05 ± 0.30	1.05 ± 0.30

Inspection level required corrected. $\alpha' = 0.05/10 = 0.005$.
* $P < 0.005$ *vs.* baseline. $\alpha'' = 0.05/3 = 0.017$.
\# $P < 0.017$ *vs.* sham group.
▲ $P < 0.017$ *vs.* saline group.

2.10. Statistical analysis

All data are reported as mean ± standard deviation. Tables 1 and 2, and Figs. 2, 4 and 5 show the results of one-way analysis of variance among the three groups. In Tables 3, 4 and 5, and Fig. 1, repeated-measures analysis of variance was used for comparison of continuous variables among multiple time points, Fisher's least significant difference test was used for comparisons between groups, and the paired *t*-test was used for comparisons within a single group. Repeated tests were corrected. A two-sided *P* value of <0.05 was considered

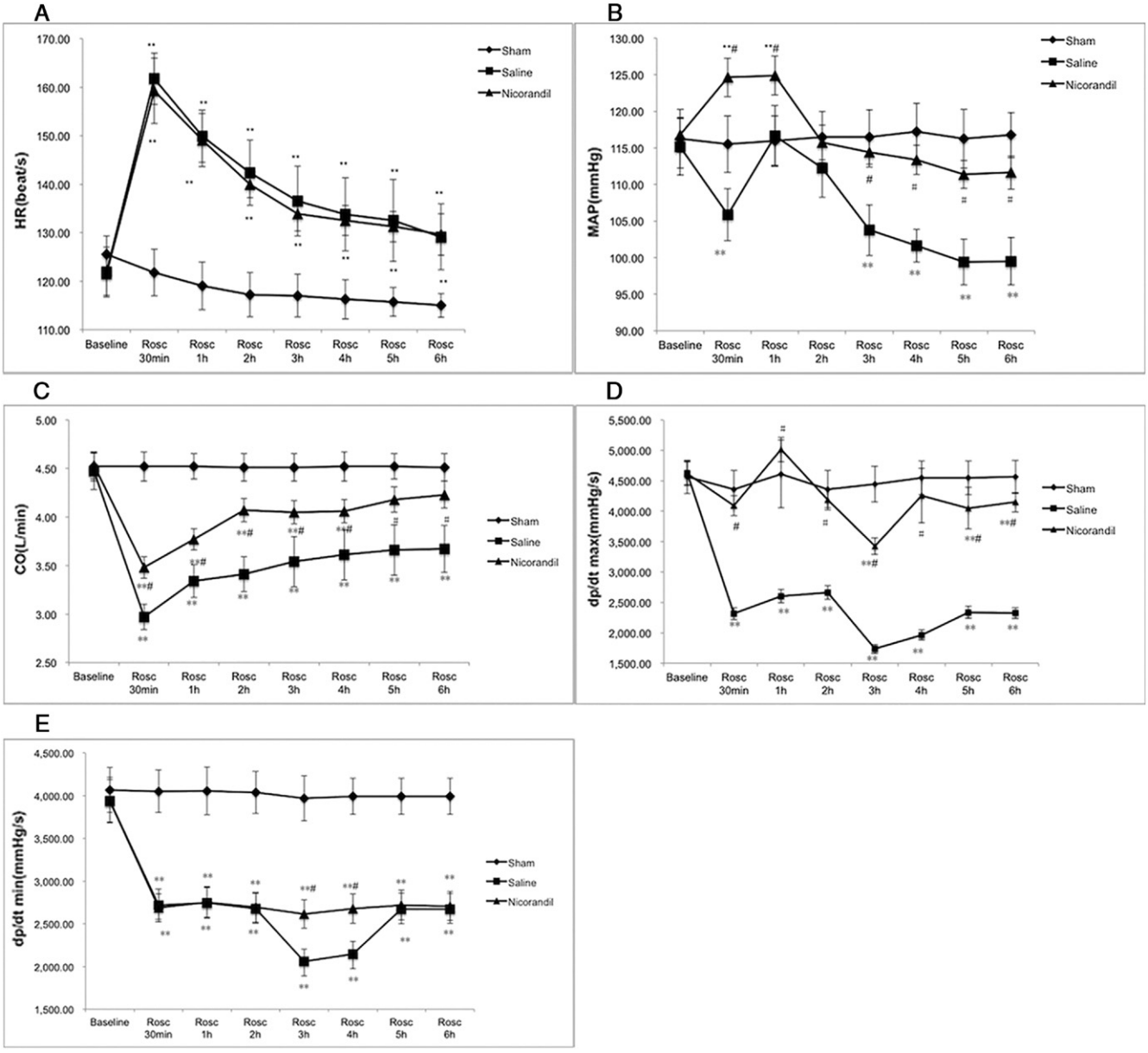

Fig. 1. Effects of nicorandil on hemodynamic parameters in the porcine model. Quantitative data of hemodynamic parameters, including left ventricular heart rate (HR), mean arterial pressure (MAP), cardiac output (CO), maximum rate of left ventricular pressure increase (dp/dtmax), and the maximum rate of left ventricular pressure decline (−dp/dtmax). Drugs were intravenously administered at onset of restoration of spontaneous circulation (ROSC). Animals were divided into sham operation (n = 4), saline control (n = 8), and nicorandil groups (n = 8). Bilateral inspection level was corrected. $\alpha'' = 0.05/3 = 0.017$. **$P < 0.017$ *vs.* sham group. #$P < 0.017$ *vs.* saline group.

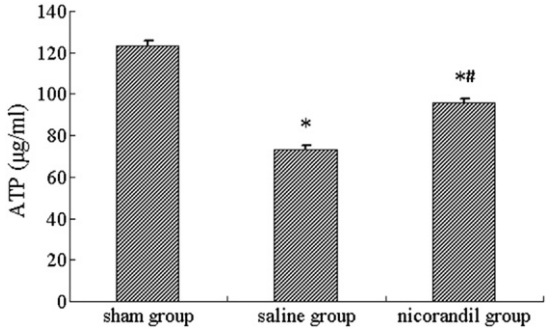

Fig. 2. Effects of nicorandil on myocardial mitochondrial ATP concentrations. $^{*}P < 0.05$ *vs.* sham group; $^{\#}P < 0.05$ *vs.* saline group.

statistically significant. All analyses were performed with statistical software (SPSS 21.0; IBM Corp., Armonk, NY, USA).

3. Results

3.1. Resuscitation outcome and baseline measurements

Sixteen animals were successfully resuscitated. There were no differences in time to ROSC, number and energy of defibrillation attempts, or epinephrine doses between the saline control and the nicorandil groups ($P > 0.05$) (Table 1). All animals survived to 6 h of ROSC. There were no differences in baseline measurements (body weight, body temperature, HR, MAP, CO, dp/dtmax, −dp/dtmax, pH, $ETCO_2$) between the three groups ($P > 0.05$) (Table 2).

3.2. Left ventricular function evaluation by invasive hemodynamic studies

After ROSC, HR was significantly higher in the saline and nicorandil groups compared with the sham group at 0.5, 1, 2, 3, 4, 5, and 6 h after ROSC ($P < 0.05$). However, there were no difference between the saline and nicorandil groups after ROSC ($P = 0.85$) (Fig. 1A). MAP was significantly lower in the saline group compared with the sham group at 0.5, 3, 4, 5, and 6 h after ROSC ($P < 0.05$), and significantly higher in the nicorandil group compared with the sham group at 0.5 and 1 h ($P < 0.05$), and with the saline group at 0.5, 1, 3, 4, 5, and 6 h ($P < 0.05$), after ROSC (Fig. 1B). CO was also significantly lower in the saline group compared with the sham group after ROSC ($P < 0.05$), and in the nicorandil group compared with the sham group at 0.5, 1, 2, 3, and 4 h ($P < 0.05$), after ROSC. However, CO was significantly increased by nicorandil post-treatment after ROSC compared with the saline group ($P < 0.05$) (Fig. 1C).

The left ventricular dp/dtmax was significantly lower in the saline than sham group ($P < 0.05$) and in the nicorandil than sham group at 3, 5, and 6 h after ROSC ($P < 0.05$). However, the left ventricular dp/dtmax was significantly higher in the nicorandil than saline group after ROSC ($P < 0.05$) (Fig. 1D). The left ventricular −dp/dtmax was significantly higher in the sham than saline and nicorandil groups at 0.5, 1, 2, 3, 4, 5, and 6 h ($P < 0.05$) and significantly higher in the nicorandil than saline group at 3 and 4 h ($P < 0.05$); however, there were no differences between the saline and nicorandil groups at 0.5, 1, 2, 5, and 6 h after ROSC (Fig. 1E).

3.3. Left ventricular function evaluation by echocardiographic studies

There were no differences in EF between the three groups at baseline. At 6 h of ROSC, EF was significantly lower in the saline and nicorandil groups compared with baseline ($P < 0.05$) and the sham group ($P < 0.05$). Further, EF was significantly higher in the nicorandil group compared with the saline group ($P < 0.05$) (Table 3).

3.4. Serum troponin, lactate, and myocardial mitochondrial ATP concentrations

There were no differences in the serum cTnI or lactate concentrations among the three groups at baseline. The serum cTnI concentration was significantly higher in the saline and nicorandil groups compared with the baseline values ($P < 0.005$) and sham group ($P < 0.05$) at 5, 30, 180, and 360 min after ROSC. The serum cTnI concentration was significantly higher in the saline than nicorandil group at 180 and 360 min after ROSC ($P < 0.05$) (Table 4). The lactate concentration was

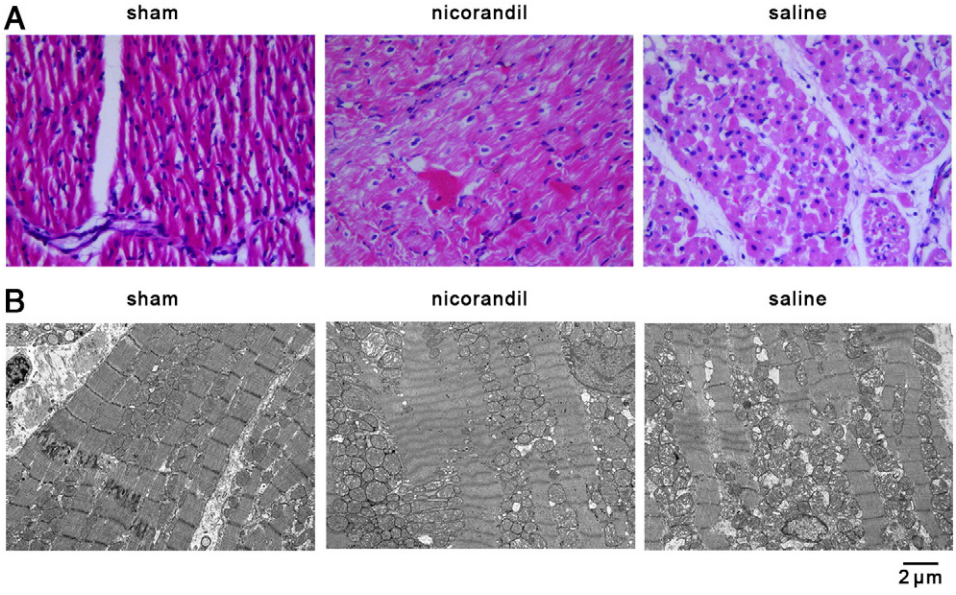

Fig. 3. Effects of saline and nicorandil on histological findings in the myocardial tissue. (A) Hematoxylin and eosin staining of myocardial tissue, sham group showing normal morphology of cardiomyocytes in the left ventricular myocardium, nicorandil group showing vacuolar degeneration, saline control group showing nuclear shrinkage, and vacuolar degeneration. (B) Cardiomyocyte mitochondrial ultrastructure, sham group showing normal cardiomyocyte ultrastructure, nicorandil group showing reduced mitochondrial swelling, saline group showing mitochondrial swelling, ridge fracture, and vacuolar degeneration.

significantly increased and peaked in the saline ($P < 0.005$) and nicorandil groups ($P < 0.005$) at 5 min after ROSC, then returned to the baseline value at 180 min after ROSC in both groups. The lactate concentration was significantly higher in the saline than nicorandil group at 5 and 30 min after ROSC ($P < 0.05$) (Table 5). These results indicate that myocardial ischemia decreased ATP synthesis (saline and nicorandil *vs.* sham group, $P < 0.05$) and that nicorandil successfully restored the concentration of ATP, preventing further deterioration (nicorandil *vs.* saline group, $P < 0.05$) (Fig. 2).

3.5. Histological analyses

Hematoxylin and eosin staining showed normal histological appearance of myocardial fibers in the sham group. In both the saline and nicorandil groups, there were similar degrees of karyopyknosis and vacuolar degeneration in myocardial cells (Fig. 3A). Transmission electron microscopy showed normal cardiomyocyte ultrastructure in the sham group. In the saline group there was evidence of myocardium damage characterized by mitochondrial congregation and severe swelling, marked ridge fracture, and vacuolar degeneration. By contrast, there was only mild mitochondrial swelling and a clear crista structure in the nicorandil group (Fig. 3B).

3.6. TUNEL assay of cardiomyocyte apoptosis

As shown in Fig. 4, the dark brown cell nuclei indicate TUNEL-positive nuclei, TUNEL staining did not show a significant apoptotic phenomenon in the sham group, whereas the number of apoptotic cells evidently increased in the saline group, and this increase was alleviated by nicorandil ($P < 0.05$).

3.7. Effects of nicorandil on the expression of Bcl-2, caspase-3 and Bax

The expression of the antiapoptotic protein Bcl-2 was significantly decreased and that of the proapoptotic protein Bax and the caspase-3 were significantly increased in the saline group compared with the sham group ($P < 0.05$). Nicorandil treatment markedly up-regulated the expression of Bcl-2 while suppressed the expression of Bax and caspase-3 compared with the saline group (all $P < 0.05$) (Fig. 5).

4. Discussion

The present study demonstrated that nicorandil successfully decreased myocardial injury in a swine model of cardiac arrest–resuscitation. The promising cardioprotective effects against myocardial injury are induced by improvements in post-ischemic myocardial dysfunction and energy metabolism, reduction of myocardial necrosis and mitochondrial damage, and inhibition of myocardial apoptosis. To the best of our knowledge, this is the first study to provide evidence of this effect of nicorandil in a model of cardiac arrest–resuscitation.

We found a marked deterioration of ventricular performance as early as 30 min after resuscitation. The compromise in left ventricular function caused a decrease in EF, CO, dp/dtmax, −dp/dtmax, and MAP. Interestingly, both left ventricular systolic and diastolic function were significantly impaired after successful ROSC, but were improved by nicorandil treatment during the initial post-resuscitation period. In support, Tang et al. reported a marked compromise in systolic and diastolic compliance at 20 min after resuscitation following a 4-min period of untreated VF in Sprague-Dawley rats [14]. In addition, we found that nicorandil, administered at onset of ROSC, can also recover post-ischemic myocardial contractile dysfunction in a porcine of cardiac arrest. In support, using an isolated rabbit heart model, Takarabe et al. [12]. reported that nicorandil treatment immediately after declamping improved contractility in cases of unexpected prolonged cardioplegic arrest. Although, nicorandil did not improve recovery of diastolic function except for 3 and 4 h after ROSC, which may relate to defibrillation of both waveform types. Indeed, diastolic function was reported to exhibit greater impairment than systolic function for both waveform types [15]. Nicorandil activates soluble guanylate cyclase *via* its nitrate-like effect, which increases cyclic guanosine monophosphate levels and KATP channel opening, leading to vasodilation of systemic veins and epicardial coronary arteries. Nicorandil was reported to increase coronary blood flow, reduce preload and afterload, and decrease MAP [16], which may contribute to the trend toward a decrease in MAP after ROSC following nicorandil in the present study. Whether nicorandil can increase coronary flow following ROSC need to be further explored.

In the present study, improved myocardial mechanical function with nicorandil could not be explained by reduced myocardial histological necrosis, as previously reported [14]. However, nicorandil treatment during reperfusion reduced mitochondrial swelling, potentially because of mitoKATP agonist activity, which may have contributed to its cardioprotective effects against oxidative damage. Indeed, nicorandil reportedly decreases IRI-induced mitochondrial swelling in the rat heart and in cardiac HL-1 cells following ischemia-reperfusion [17]. A cardioprotective role of nicorandil is also supported by the reduction in serum cTnI, a specific myocardial injury marker, after ROSC in our study. Oxidative phosphorylation is the major method of ATP generation. Lactate is produced by anaerobic glycolysis when the metabolic demand for oxygen exceeds the available oxygen supply. Once mitochondrial dynamics are damaged, ATP generation decreases. In the present study, the lactate concentration was increased in the saline and nicorandil groups after ROSC, and nicorandil treatment reduced the lactate concentration at 5 and 30 min after ROSC. The ATP concentration was significantly decreased in the saline and nicorandil groups and nicorandil successfully restored the concentration of ATP, preventing further deterioration. These results indicate that myocardial global ischemia after cardiac arrest increases the lactate concentration immediately, aggravates mitochondrial deficits and decreases the ATP concentration. Administration of nicorandil after ROSC ameliorated these negative effects and increased the ATP concentration. Speculatively, this may be associated with the hemodynamic effects of nicorandil, which occur within 1 to 2 min of intravenous administration [18], resulting in preservation of cellular energy metabolism and the redox state, and improved mitochondrial function. Therefore, our study suggests that nicorandil may also produce cardioprotective effects by improvements in energy metabolism. In support of this suggestion, one study revealed that the effects of nicorandil on mitoKATP channels preserved cellular energy metabolism and the redox state and prevented mitochondrial permeability transition pore formation; opening of these pores is a common pathway for cellular apoptosis and death after injury [19].

Apoptosis is a mainstay of tissue damage secondary to reperfusion injury after a short period of ischemia. Studies have suggested that the upregulation of several antiapoptotic genes including Bcl-2 and downregulation of proapoptotic genes such as Bax play an important role in salvage of ischemic tissue [20]. Downregulation of Bcl-2/Bax might result in activation of the caspase family of proteases, such as caspase-3, which is responsible for the induction of apoptotic cell death [21]. TUNEL staining showed that the number of TUNEL-positive cells was significantly lower in the group treated with nicorandil than in the saline group. We also observed that nicorandil treatment decreased Bax and caspase-3 expression and increased Bcl-2 expression compared with the saline group. These results indicate that nicorandil exerted remarkable cardioprotective effects against myocardial injury following cardiac arrest and resuscitation through the effects of antiapoptosis.

Nicorandil is both a mitochondrial and sarcolemmal KATP agonist. A previous study demonstrated that pharmacological preconditioning and post-conditioning with nicorandil attenuated ischemia–reperfusion-induced myocardial injury by opening mitoKATP channels [22]. Other studies have provided direct evidence that the preconditioning-like effect of KATP channel antagonists in the heart can be exerted at

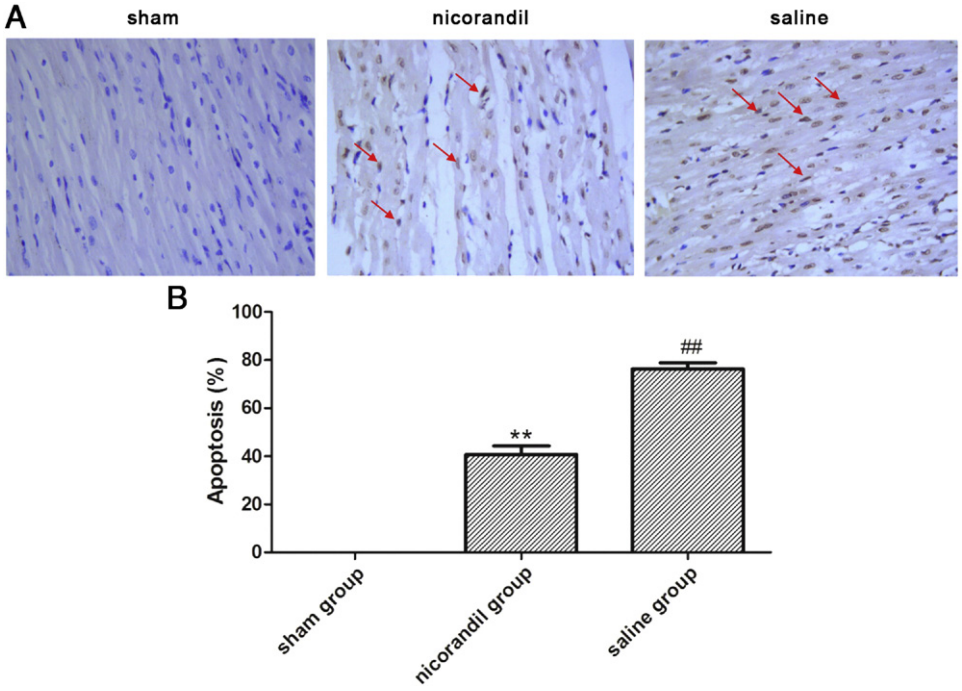

Fig. 4. Effects of nicorandil suppression on cardiomyocyte apoptosis (×400). A: Representative immunohistochemical staining for apoptotic cell (which were manifested as a marked appearance of dark brown cell nuclei, as the red arrows noted) in rat myocardium in the different groups. B: Quantitative measurement of the TUNEL index (apoptosis %) in different groups. $^{**}P < 0.05$ *vs.* saline group; $^{\#\#}P < 0.05$ *vs.* sham group.

the level of cardiac myocytes and is most likely the result of KATP channel activation [14,23,24,25]. The effect of KATP channels has been extensively studied, and KATP agonists and antagonists have shown both benefit and harm in models of ischemic preconditioning [23,24,25]. Cardiac KATP channels are also extremely important in arrhythmia substrates during cardiac ischemia. Opening of KATP channels induces action potential shortening, and in the acute phase may worsen arrhythmia substrates [26]. Conversely, KATP channel blockade using drugs such as glibenclamide may improve resuscitation from VF [27]. Although the initial success rate of CPR is 40% in settings of out-of-hospital cardiac arrest, a majority of these patients die within 72 h, primarily of heart failure and/or recurrent VF. Further studies are required to determine whether the cardioprotective effects of nicorandil against myocardial injury following cardiac arrest are related to opening of the KATP channels and elucidate the effect of KATP channels on arrhythmias after ROSC.

This study has several limitations. First, experiments were performed on healthy pigs without cardiovascular disease, and cardiac

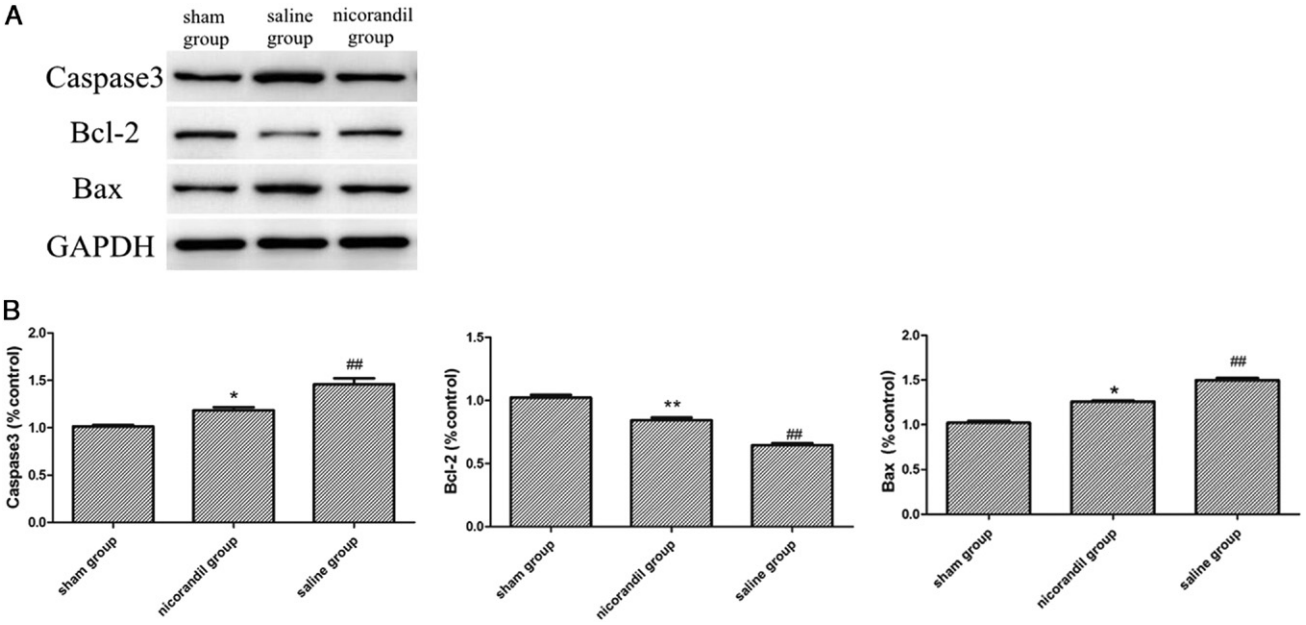

Fig. 5. Western blotting analysis of Bcl-2, Bax and caspase-3. GAPDH was used to demonstrate equal protein loading. A: Representative images are shown. B: Quantitative measurement of the Western blot (% control) in different groups . $^{**}P < 0.01$ *vs.* saline group; $^{*}P < 0.05$ *vs.* saline group; $^{\#\#}P < 0.01$ *vs.* sham group.

arrest was induced by acute VF, whereas most humans with cardiac arrest are not healthy. Second, the sample size was small, with only eight surviving animals. Finally, we did not determine the protective mechanism of IRI with the effects of nicorandil on mitoKATP channels.

In conclusion, our data suggest that nicorandil can reduce the severity of post-resuscitation myocardial injury caused by ischemia-reperfusion following cardiac arrest. We have provided the first evidence that treatment with nicorandil exerts significant cardioprotective effects through improvement of heart function, reduction of myocardial necrosis, and inhibition of myocardial apoptosis. Further studies are required to determine the optimal dosage and time window for effective treatment with nicorandil.

Funding

This work was supported by the 2012 Jinan Science and Technology Development Plan [grant numbers 201219007] and National Natural Science Foundation of China [grant numbers 81471833].

Acknowledgments

We thank Dr. Nan-Zhang for technical assistance.

References

[1] Nadkarni VM, Larkin GL, Peberdy MA, Carey SM, Kaye W, Mancini ME, et al. First documented rhythm and clinical outcome from in-hospital cardiac arrest among children and adults. JAMA 2006;295:50–7.
[2] Shan Y, Ristagno G, Fuller M, Sun S, Li Y, Weil MH, et al. The effects of phase duration on defibrillation success of dual time constant biphasic waveforms. Resuscitation 2010;81(2):236–41.
[3] Zhang Q, Li CS. Combination of epinephrine with esmolol attenuates post-resuscitation myocardial dysfunction in a porcine model of cardiac arrest. PLoS One 2013; 8(12):e82677.
[4] Geocadin RG, Peberdy MA, Lazar RM. Poor survival after cardiac arrest resuscitation: a self-fulfilling prophecy or biologic destiny? Crit Care Med 2012;40:979–80.
[5] Zhao ZG, Tang ZZ, Zhang WK, Li JG. Protective effects of embelin on myocardial ischemia-reperfusion injury following cardiac arrest in a rabbit model. Inflammation 2015;38(2):1–7.
[6] Kern KB. Postresuscitation myocardial dysfunction. Cardiol Clin 2002;20:89–101.
[7] Laurent I, Monchi M, Chiche JD, Joly LM, Spaulding C, Bourgeois B, et al. Reversible myocardial dysfunction in survivors of out-of-hospital cardiac arrest. J Am Coll Cardiol 2002;40:2110–6.
[8] Ruiz-Bailén M, Aguayo de Hoyos E, Ruiz-Navarro S, Díaz-Castellanos MA, Rucabado-Aguilar L, Gómez-Jiménez FJ, et al. Reversible myocardial dysfunction after cardiopulmonary resuscitation. Resuscitation 2005;66:175–81.
[9] Kilgannon JH, Roberts BW, Reihl LR, et al. Early arterial hypotension is common in the post-cardiac arrest syndrome and associated with increased in-hospital mortality. Resuscitation 2008;79:410–6.
[10] Trzeciak S, Jones AE, Kilgannon JH, Chansky ME, Jones AE, Dellinger RP, et al. Significance of arterial hypotension after resuscitation from cardiac arrest. Crit Care Med 2009;37:2895–903.
[11] Wu H, Ye M, Yang J, Ding J, Yang J, Dong W, et al. Nicorandil protects the heart from ischemia/reperfusion injury by attenuating endoplasmic reticulum response-induced apoptosis through PI3K/Akt signaling pathway. Cell Physiol Biochem 2015; 35(6):2320–32.
[12] Takarabe K, Okazaki Y, Higuchi S, Murayama J, Natsuaki M, Itoh T. Nicorandil attenuates reperfusion injury after long cardioplegic arrest. Asian Cardiovasc Thorac Ann 2007;15(3):204–9.
[13] Kleinman ME, Brennan EE, Goldberger ZD, Swor RA, Terry M, Bobrow BJ, et al. Part 5: adult basic life support and cardiopulmonary resuscitation quality: 2015 American Heart Association guidelines update for cardiopulmonary resuscitation and emergency cardiovascular care. Circulation 2015;132(18 Suppl 2):S414–35.
[14] Tang WC, Weil MH, Sun S, Pernat A, Mason E. KATP channel activation reduces the severity of postresuscitation myocardial dysfunction. Am J Physiol Heart Circ Physiol 2000;279:H1609–15.
[15] Leng CT, Paradis NA, Callkins H, Berger RD, Lardo AC, Rent KC, et al. Resuscitation after prolonged ventricular fibrillation with use of monophasic and biphasic waveform pulses for external defibrillation. Circulation 2000;101:2968–74.
[16] Horinaka S. Use of nicorandil in cardiovascular disease and its optimization. Drugs 2011;71(9):1105–19.
[17] Raquel S, Carreira PM, Gonçalves LM, Providência LA. Nicorandil protects cardiac mitochondria against permeability transition induced by ischemia-reperfusion. J Bioenerg Biomembr 2008;40:95–102.
[18] Frampton J, Buckley MM, Fitton A. Nicorandil: a review of its pharmacology and therapeutic efficacy in angina pectoris. Drugs 1992;44(4):625–55.
[19] Lamarche F, Carcenac C, Gonthier B, Cottet-Rousselle C, Chauvin C, Barret L, et al. Mitochondrial permeability transition pore inhibitors prevent ethanol-induced neuronal death in mice. Chem Res Toxicol 2012;26(1):78–88.
[20] Qu D, Han J, Ren H, Yang W, Zhang X, Zheng Q, et al. Cardioprotective effects of astragalin against myocardial ischemia/reperfusion injury in isolated rat heart. Oxidative Med Cell Longev 2016;2016:8194690.
[21] Zhang Q, Wang G, Yuan W, Wu J, Wang M, Li C. The effects of hosphodiesterase-5 inhibitor sildenafil against post-resuscitation myocardial and intestinal microcirculatory dysfunction by attenuating apoptosis and regulating micrornas expression: essential role of nitric oxide syntheses signaling. J Transl Med 2015;13:177.
[22] Li W, Wu N, Shu WQ, Jia DL, Jia PY. Pharmacological preconditioning and postconditioning with nicorandil attenuates ischemia/reperfusion-induced myocardial necrosis and apoptosis in hypercholesterolemic rats. Exp Ther Med 2015;10(6): 2197–205.
[23] Fryer RM, Hsu AK, Eells JT, Nagase H, Gross GJ. Opioid-induced second window of cardioprotection potential role of mitochondrial KATP channels. Circ Res 1999; 84(7):846–51.
[24] Gross GJ, Fryer RM. Sarcolemmal versus mitochondrial ATP-sensitive K^+ channels and myocardial preconditioning. Circ Res 1999;84:973–9.
[25] Liang BT, Gross GJ. Direct preconditioning of cardiac myocytes via opioid receptors and KATP channels figure legends. Circ Res 1999;84:1396–400.
[26] Carmeliet E. Cardiac ionic currents and acute ischemia:from channels to arrhythmias. Physiol Rev 1999;79(3):917–1017.
[27] Taylor TG, Venable PW, Shibayama J, Warren M, Zaitsev AV. Role of KATP channel in electrical depression and asystole during long-duration ventricular fibrillation in ex vivo canine heart. Am J Physiol Heart Circ Physiol 2012;302(11):H2396–409.